TPM Vol. 32, No. S4, 2025
ISSN: 1972-6325
https://www.tpmap.org/

SOFTMAX LOGICAL GATED CONVOLUTIONAL NEURAL NETWORK FOR EFFICIENT AND ACCURATE DETECTION OF MULTIPLE MYELOMA IN MICROSCOPIC IMAGES

[1*]DHIYANESH B, [2]AUGUSTA KANI G, [3]SARASWATHI P, [4]RAMESH B, [5]CHOKKANATHAN L

[1*]ASSOCIATE PROFESSOR/ CSE ETECH, SRM INSTITUTE OF SCIENCE AND TECHNOLOGY, VADAPALANI CAMPUS, CHENNAI, TAMIL NADU INDIA.
[2]ASSISTANT PROFESSOR/ CSE ETECH, SRM INSTITUTE OF SCIENCE AND TECHNOLOGY, VADAPALANI CAMPUS, CHENNAI, TAMIL NADU INDIA.
[3]ASSISTANT PROFESSOR/IT, VELAMMAL COLLEGE OF ENGINEERING AND TECHNOLOGY, MADURAI, TAMIL NADU, INDIA.
[4]ASSOCIATE PROFESSOR/ECE, ANNAPOORANA ENGINEERING COLLEGE, SALEM, TAMIL NADU INDIA.
[5]ASSOCIATE PROFESSOR/AI & DS, MADANAPALLE INSTITUTE OF TECHNOLOGY AND SCIENCE, MADANAPALLE, ANDHRAPRADESH.
[1*]dhiyanu87@gmail.com, [2]augus.jesus@gmail.com, [3]psaraswathimtech@gmail.com, [4]mailrameshece@gmail.com, [5]gokiladeepagopal@gmail.com

Abstract
A malignant tumor of plasma cells and multiple myeloma has complicated the disorders. These multiple myeloma images were taken microscopically. The process is time-consuming and labor-intensive, so it results in some noisy images. Identifying cancer cells is difficult and provides less accuracy due to noise in the images. To overcome the above problem, the Softmax Logical Gated Convolutional Neural Network (SLGCNN) approach was applied. The first step is to filter the multiple myeloma by implementing a Median Image Filter based Edge Detection (MIFED). The second stage divides the multiple myeloma preprocessed images using Screen Cluster Area Segmentation (SCAS) enhancing image clarity by eliminating irrelevant parts. After segmentation, we used Recurrent Feature Elimination (RFE) to achieve the selection of an essential set of features to decrease the number of features making processing faster without a loss of efficiency. Moreover, a SLGCNN is employed for the final classification of the refined features, due to its capacity for logical gating that enables the distinction between cytoplasm and nucleus cells with high accuracy. This methodology solves the problems of the and makes this approach to detecting multiple myeloma computationally efficient and clinically valid. The proposed framework could contribute to early intervention and improve the results of multiple myeloma patients by increasing the reliability of diagnosis. The proposed method archives a high accuracy of 96.8% compared to the other systems.

Keywords: Multiple Myeloma, Microscopic Images, Median Image Filter, Edge Detection Area Segmentation, Cancer Cell, Clinical Diagnosis, Cytoplasm and Nucleus Differentiation

1. INTRODUCTION

In the past, multiple myeloma (MM) was an incurable B-cell malignancy characterized by the proliferation and growth of clonal plasma cells in the bone marrow [1]. When MM is identified, 80% of patients have osteolytic lesions. The axial skeleton's proximal long bones and vertebrae are the most often impacted. In recent years, imaging techniques and improved medical and non-pharmacological treatments have improved the performance of the underlying pathophysiological framework to protect the patient affected by myeloma-associated bone disease (MBD), which can have a profound impact on morbidity and quality of life. According to the Visual Image Analysis and Processing Department, leukemia is defined as the percentage of red or white blood cells in a plasma sample [2]. etiquette-free methods.

MM is an incurable hematological cancer caused by the clonal growth of plasma cells. The bone marrow frequently contains malignant plasma cells, which generate aberrant antibodies (M protein). In economically developed nations, the lifetime risk of MM is between 0.6 and 1%, and over 140,000 cases are diagnosed globally each year. Patients are identified based on conventional diagnostic methods for MM, such as clinical analysis,

bone marrow biopsy, and radiological evaluation [3-5]. As a result, detecting test results while implementing new techniques to achieve a quick, economical, and accurate identification of MM is time-consuming and costly. In recent years, laser-induced breakdown spectroscopy (LIBS) has been used in a variety of biomedical materials, including tumor tissues, soft tissues, and bioaerosols. A new method in biomedical applications is the combination of machine learning methods and blood sample-based LIBS for the identification and diagnosis of malignant tumors. These tumors are characterized by monoclonal immunoglobulins and the buildup and clonal growth of cancerous plasma cells in the bone marrow.

MM is the second most common hematologic malignancy among diseases involving abnormal plasma cells. Due to the development of immunomodulators and proteasome inhibitors, the survival rate of MM patients has improved significantly over the past decade. Comprehending the underlying mechanisms and novel targets causing disease development and recurrence in MM is crucial to enhancing treatment and prognostic prediction [6-7]. The treatment of MM has changed in recent years with the introduction of proteasome inhibitors, immunomodulators, histone deacetylase inhibitors, and monoclonal antibodies.

Subsequently, it has been demonstrated that MM cells and cells in the surrounding bone marrow environment react to medications when myeloma cells' biological behavior changes. Direct adhesion contributes to drug resistance by leading to the emergence of survival signals [8]. Clarifying the molecular systems involved in Cell Adhesion-Mediated Drug Resistance (CAM-DR) may support identifying new therapeutic strategies to address this issue. Furthermore, stroma-induced defences, secreted soluble factors, and Bone marrow stromal cells (BMSCs) contribute to drug resistance in associated MM.

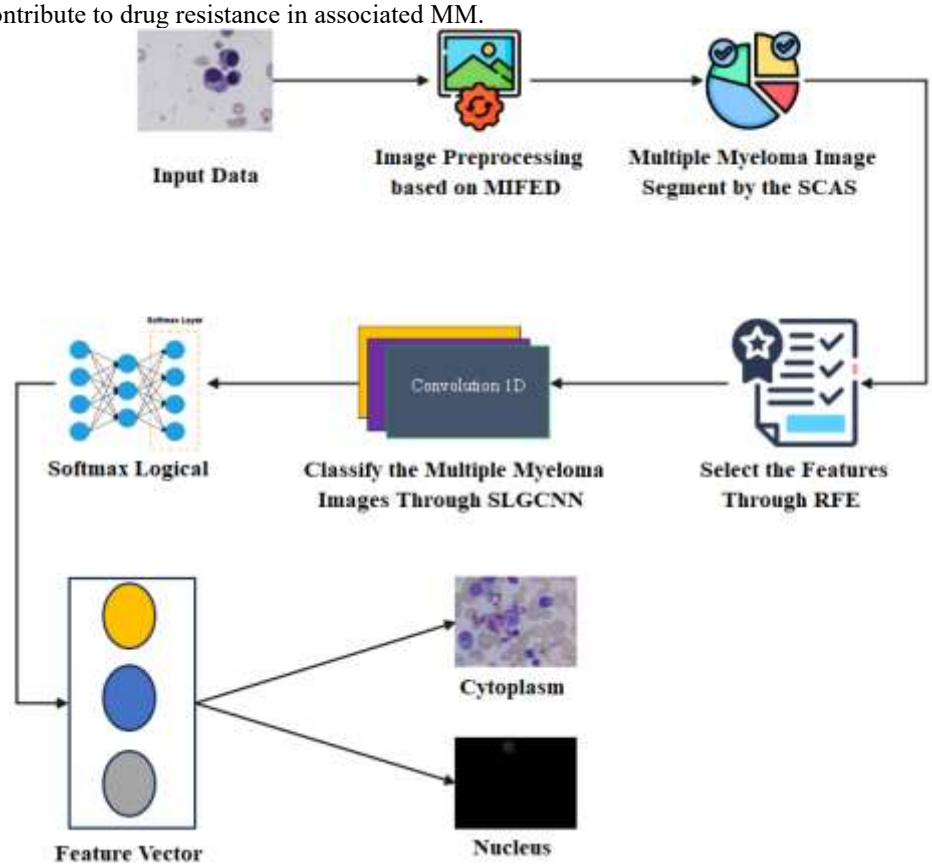

Figure 1. Diagram of the phases and its working process of the proposed method

However, lytic bone lesions, which result in pathological fractures and excruciating pain, are an indicator of bone disease in MM patients. Moreover, compared to physiological bone transformation, bone creation takes place in areas of bone resorption. Severe dysfunction of osteoblasts is marked by increased local osteolysis or suppression in areas adjacent to MM Bone Disease (MMBD) cells. Systemic bone loss and nonhealing lytic bone lesions are the outcomes of this combo. Additionally, MMBD can lead to bone fractures and rapid tumor growth, both of which decrease survival rates [9-10]. Similarly, conventional testing methods require a lot of resources, which makes extending challenging. In addition to restricting the capacity to expand diagnostic facilities in remote areas, they necessitate costly medical infrastructure and skilled personnel to inspect.

2. LITERATURE SURVEY

Complete blood cell counts and myeloma plasma cell counts on aspirate slide images are two techniques for MM detection in bone marrow [11]. These manual detection methods require a lot of time, and the pathologist's experience determines the final result.

The novel proposed a new identification technique for myeloma-infected plasma cells [12]. According to experimental results on the SegPC dataset, the suggested deep learning (DL) approach performs better in myeloma diagnosis and detection than other competing approaches.

Using existing MM imaging data, a convolutional neural network (CNN) model is built and evaluated by inputting classified image data to verify its accuracy [13]. Furthermore, CNN improves diagnostic performance by leveraging the depth of field to detect medical images.

The effect of different chemotherapy regimens on patient prognosis was investigated using a suggested Regional CNN (RCNN) model [14]. It was established that various chemotherapy regimens affected the prognosis of patients utilizing a DL-based model segmented myeloma CT images.

The novel proposed a two-stage DL model that incorporates bone segmentation and subsequent damage detection. Correspondingly, it suggests "You Look Only One" (YOLO) models for damage detection and bone segmentation.

Using accurate and rapid segmentation techniques, doctors can diagnose diseases and treat patients more effectively and quickly [16]. Algorithms like a multilayer perceptron and a novel composite histogram-based smooth-covered rough k-means clustering technique are used in preprocessing.

The author [17] described Machine Learning (ML) algorithms designed for MM clinical and RNA sequencing data collected by the CoMMpass consortium. They developed a random forest model with 50 variables that consistently predicted overall survival across both training and validation sets.

A hybrid multi-objective and category-based optimization technique is used to adaptively optimize hyperparameters in the deep CNN architecture that was described [18]. However, because a pathologist must identify the specimen, manual specimen identification is delicate and time-consuming, delaying prompt diagnosis and treatment.

Then, an optimized Dense CNN (DCNN) architecture is used to train the model and eventually predict the type of cancer within the cell [19]. Models are trained on cell images, first pre-processing images to extract the optimal features.

The author [20] proposed a suitable framework for MM diagnosis using microscopic blood cell image data, which addresses our proposed key challenges of visual similarity between healthy cell types and cancer cell types and label noise.

Table 1. Multiple Myeloma Based on Image Processing using machine learning

Author	Classification	Performance Evaluation	Limitation	Accuracy
Zbigniew Omiotek [21]	K-Nearest Neighbour (K-NN)	positive predictive value, Sensitivity, accuracy	When the healthy cells are replaced, the bone is destroyed.	93%
Shobana M [22]	Fuzzy Support Vector Machine (FSVM)	Accuracy, Sensitivity, Specificity	The majority of patients in the advanced stage become resistant to therapy.	91.5%
Guilal,[23]	Random Forest (RF)	Accuracy	The diagnostic process is time-consuming since it is hard to identify in its early stages.	72%
Cai [24]	SVM	sensitivity, specificity	The prevalence of multiple myeloma is rising worldwide.	77%
Aarthy, R [25]	Gated CNN (GCNN)	Precision, recall and F-measure	Because of the noise in the images, conventional methods are unable to detect cancer cells.	83%
Yu [26]	Mask Region–Based CNN (Mask R-CNN)	Recall, Precision	An automated differential technique that can be used in clinical settings is not provided.	88%
Xiong X [27]	Artificial Neural Networks (ANN)	Matthew's correlation	When bone marrow analysis becomes part of medical	0.648%

		coefficient (MCC), sensitivity	practice, it causes fractures in patients.	
Ubels J [28]	Simulated Treatment Learned Signatures (STLsig),	Sensitivity	Proteasome medicine's possible advantages for MM patients must be evaluated.	0.91%

Patients with advanced myeloma had more stage 1 features ($p < 0.02$), yet stage 2 "Grey Level Co-Occurrence Matrix (GLCM) clusters were significant." Histology and serological factors associated with myeloma exhibit a strong correlation with CT structural features applied to non-calcium bone marrow imaging [29]. The author [30] discussed the overall accuracy when training using the optimal Dense CNN (DCNN) model, with a final prediction rate of 91.2% for intracellular cancer types.

3. MATERIALS AND METHODS

In this section we briefly described about the proposed method. In this proposed method we execute the four phases: preprocessing, segmentation, feature selection, and classification. In this first phase we use MIFED, in the second phase we SCAS, at the third phase RFE, and the final phase we use SLGCNN method. For classify the multiple myeloma with high accuracy we use SegPC-2021-dataset, and it is taken from Kaggle website.

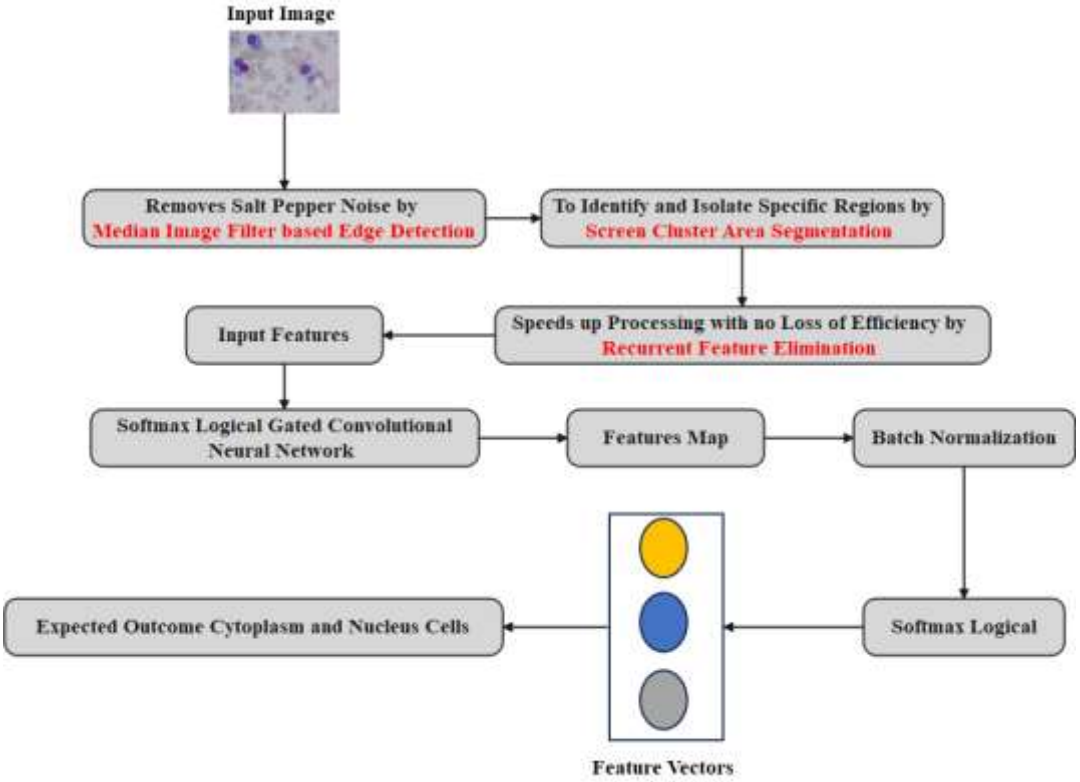

Figure 2. Architecture diagram of the of the proposed method

In figure 2 we illustrate the architecture diagram of the deployed methodology. The MIFED technique removes high-frequency noises like salt and pepper noise, which makes it appropriate for improving image quality, especially in medical imaging, without improving the smoothing of important structures. SCAS is used to identify and isolate specific regions in medical images that may include cancerous cells in order to segment images of multiple myeloma. The SCAS technique is a system for segmenting images of multiple myeloma into smaller, easier-to-manage portions or "clusters" based on specific criteria or attributes. The RFE technique, which reduced the amount of features and speeds up processing with no loss of efficiency, is then used to pick a critical set of features. For the final classification of the enhanced features, an SLGCNN is used because of its ability to perform logical prohibiting, which allows for an high level of accuracy in differentiating between cytoplasm and nucleus cells.

3.1 Dataset Description

We employ the SegPC-2021 dataset, obtained from the Kaggle website, to precisely categorize multiple myeloma. The training set, validation set, and final test set, which are all used for the challenge, are contained in the data folder. The GT is not available for the test set, but it is for the train and validation sets. Using bone marrow aspirate slides, microscopic pictures of patients with Multiple Myeloma (MM), a kind of white blood malignancy, were taken. Plasma cells, or cells of interest, need to be segmented, and slides were stained with Jenner-Giemsa stain. Figure 3 shows example pictures of the cytoplasm and nucleus of multiple myeloma cells.

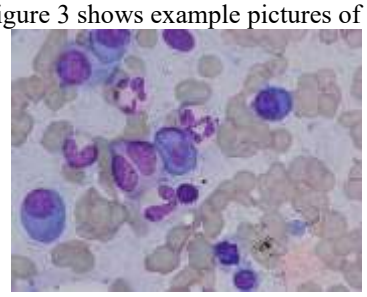

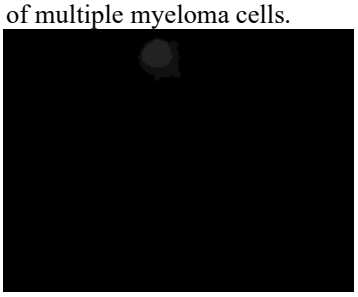

Figure 3(a) Sample image of cytoplasm cell Figure 3 (b). Sample image of nucleus cells

There are 298 images in throughout the dataset. The GT for the cell of interest has been supplied in subfolder y (under the train folder) for every image in subfolder x (under the train folder). Although GT is only available for cells of interest, there may be more cells as well. Only the cells of interest will be used to test performance during evaluation. As a result, the algorithm's performance on the cells of interest will be the sole basis for ranking. Only the cells of interest that we have pre-identified will be taken into account by the evaluation algorithm.

3.2 Median Image Filter based Edge Detection (MIFED) method

The median image filter, is one of the most precious tools for removing the noise from the images. The median filter is another method of FFT that works by sliding a window (kernel) over the image and replacing each pixel in the window with the value of the median of the pixels in that window when the images of SegPC-2021-dataset were undergoing preprocessing. This process assists in preserving edges in addition to removing salt and pepper noise and other high-frequency noises, and that is why it is appropriate, especially in medical imaging, to improve image quality without enriching the smoothening of essential structures. The MIFED method is computed through the equation 1,

$$j(x,y) = \mu i(I,1): \quad (I,1) \in U(x,y) \tag{1}$$

Let assume, I as image, x, y as the position $j(x,y)$ as output pixel price at place, μ as median, and U as the predetermined window length. This equation enables to do away with salt and pepper noise from the microscopic images even as preserving the important diagnostic facts. After that while decreasing noise inside the image the hold the edges and information through equation 2,

$$j(x,y) = U(x,y) \sum m = -r \sum o = -r f_{q(x-I,y-o) f_{m(i(x,y)-i(I,0))i(I.o)}} \tag{2}$$

Let assume, m, o as variety weighting function, $f_q(x,y)$ as the spatial weighting feature. The equation 2 is used to hold edges and info within the image while reducing noise. In equation 3 we enhance the first-rate of the microscopic images,

$$U(x,y) = \sum I = -r \sum 1 = -r f_{q(x-N,y-o) f_{m(i(x,y)-i(k,o))}} \tag{3}$$

This equation enhances the first-rate of the microscopic images and decorate the overall performance of the SegPC-2021-dataset images. By the following equation 4 we detect the edges,

$$D(i,j) = \sqrt{(D_i)^2 + \left(D_j\right)^2} \tag{4}$$

Let assume, i, j as pixel, $(D_i)^2$ as gradient addition horizontal axes, and $\left(D_j\right)^2$ as vertical axes, after detect the edges we compute the gradient path through equation 5,

$$\theta(i,j) = tan^{(-1)\left(\frac{D_j(i,j)}{D_i(i,j)}\right)} \tag{5}$$

It extends the basic Sobel operator by adopting a scale-area technique, which enhances the recognition of edges by smoothing the picture at some Gaussian clear-out at one or additional scales. This enables to reduction of the noise inside the image and boosts the brink detection efficiency. The scale area is applied after overlaying the picture with a Gaussian clear-out at distinctive scales, after which determining the gradient significance and direction at each scale. In the case of the SegPC-2021 dataset, employing a MIFED assists in enhancing the overall nature of images for the target disease, and riding such deep learning form features related to the disease.

3.3 Screen Cluster Area Segmentation (SCAS) method

For multiple myeloma image segmentation, Screen Cluster Area Segmentation (SCAS) entails locating and separating the precise areas in medical pictures that might contain malignant cells. The SCAS approach divides the image into smaller, more manageable segments or "clusters" according to particular criteria or qualities. This method allows for more precisely identifying and isolating the regions of interest linked to multiple myeloma cells or lesions. In equation 6 we maximizing the intensity values in the image,

$$S = argmax_s\{Q(s)\} \quad (6)$$

Let assume, S as threshold, $Q(s)$ as the intensity values in the image. It is used to separating background and potential multi myeloma clusters. It is often determined via algorithms like Otsu's method. By following the equation 7 we classify the pixels,

$$min \sum_{x=1}^{k} \sum_{i \in D_x} \|i - \mu_x\|^2 \quad (7)$$

Let assume, i as pixels, D as cluster, μ_x as centroid of each D, and k as k-means clustering partitions pixels. This equation is used to highlight possible myeloma regions based on similarity in pixel intensities. After highlight the possible myeloma regions we compute the region growing based on segmenting cluster areas through equation 8,

$$R = \bigcup_{q \in N}\{q \| \|X(q) - X(r)\| < \epsilon\} \quad (8)$$

Let assume, R as region, X as intensity, r as initial seed, and ϵ as threshold. This equation is used to isolate contiguous areas associated with multiple myeloma lesions. By following we set the level for boundary detection through equation 9,

$$\frac{\partial \emptyset}{\partial s} = \delta(\emptyset)\left(\alpha \nabla . \left(\frac{\nabla \emptyset}{|\nabla \emptyset|}\right) + \beta\right) \quad (9)$$

The level set function ϕ evolves over time s to detect boundaries of regions. This equation balances contour smoothing (first term) with boundary adherence (second term), identifying precise borders around clusters in the segmented image. In equation 10 we perform the post-segmentation morphological operations,

$$X_c = (X \ominus E) \oplus E \quad (10)$$

Let assume, X as input image, E as structuring element, $\ominus$ as erosion, and $\oplus$ as dilation. In this equation $\ominus$ and $\oplus$ are applied to refine segmented areas by removing small artifacts or filling holes, where E is a structuring element. These helps clean up the final segmented clusters, enhancing segmentation accuracy for multiple myeloma areas. Then we compute the Dice Similarity Coefficient G through equation 11,

$$G = \frac{2|I \cap J|}{|I| + |J|} \quad (11)$$

Here, I, J is represent for sets of pixels in the segmented region and the ground truth. The equation 11 is a common metric used to evaluate the accuracy of segmentation. It measures how well the segmented clusters match with true multiple myeloma regions, providing a score from 0 (no overlap) to 1 (perfect overlap).

3.4 Recurrent Feature Elimination (RFE) method

RFE is an iterative approach to choosing features since it involves recycling and iteratively using the feature selection model repeatedly. Based on the image data, a predictive model is developed to assess the importance of each of the features in question. They, of course, could be pixel intensities, texture patterns, or other extracted higher-level features. In this RFE it seems that the features are ordered according to the relevance, it often turns out the numbers right from the weights, coefficients or contribution scores. The feature that contributes the least to the model is removed, and the process reiterates until all the features are removed and the model is rebuilt. The process continues till the best set of features is brought into focus in order to eliminate overlapping features and also increase the speed of computational ability and generalization of the best model. RFE is most suitable for medical image analysis tasks such as multiple myeloma detection since it assists the model in paying attention to the relevant features and consequently increases the model's accuracy and interpretability. In equation 12 we compute the feature importance score,

$$X(f_x) = \frac{\partial \mathcal{L}}{\partial f_x} \quad (12)$$

Let assume, X as importance score, f_x as feature, $\frac{\partial \mathcal{L}}{\partial f_x}$ as loss function, and $\frac{\partial \mathcal{L}}{\partial f_x}$ as gradient of the $\mathcal{L}$ with respect to the f_x. The feature importance is calculated based on the contribution of each feature to the predictive model. This equation compute how sensitive the $\mathcal{L}$ is to changes in f_x, indicating its significance. By following we perform the criterion of the recursive elimination through the equation 13,

$$E(i) = \{f_x | X(f_x) \leq T(i)\} \quad (13)$$

Let assume, E as eliminated features, i as iteration, T as threshold it is minimum importance score for retaining a feature in i. In this equation in each iteration, features with the least importance scores are eliminated. Then, it removes less relevant features iteratively to refine the feature subset. After eliminated the least importance scores, we retraining the model through equation 14,

$$\hat{j} = f(X_i) \quad (14)$$

Let assume $\hat{j}$ as predicted output, f as model, X_i as reduced feature set after the i. The equation is adjusting to the new feature subset, improving the reliability of feature importance scores. After improving the reliability of feature importance scores, features are ranked based on their elimination order or final importance scores, so we ranking the features through equation 15,

$$R(f_x) = i(f_x) \quad (15)$$

In this equation assigns higher ranks to features retained longer, indicating greater importance. By following we stopping the criterion through equation 16,

$$\Delta P < \epsilon \quad (16)$$

Let assume P as performance, ΔP as change in performance metric between successive i, and ϵ as tolerance T. The process stops when a predefined number of features remain or performance metrics. This equation avoids over-elimination and ensures the optimal subset of features is selected. To choose the best-performing feature subset on the provided data, RFE iteratively removes irrelevant features and assesses model performance via cross-validation. This reduces the possibility of overfitting while improving the model's ability to generalize.

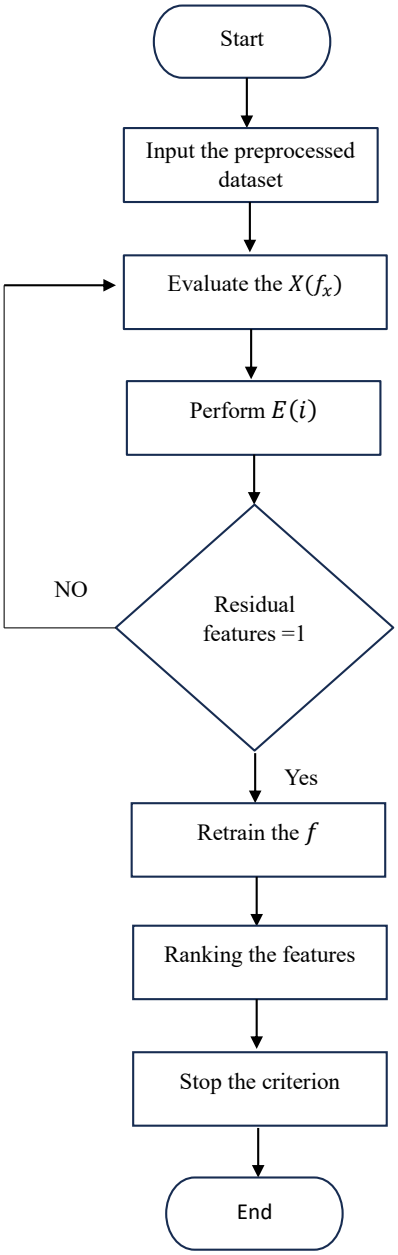

Figure 4. Flowchart Diagram of the RFE method

In figure 4 we illustrate the work flow diagram of the RFE method. In this RFE method we first input the preprocessed dataset which containing multiple myeloma images. After we evaluate the feature importance

score $X(f_x)$, then perform the criterion of the recursive elimination, if residual features is equal to 1 retrain the function, else again evaluate the $X(f_x)$. After retrain the model assigns higher ranks to features retained longer, indicating greater importance. Last, we stopping the criterion to avoids over-elimination and ensures the optimal subset of features is selected.

3.5 Softmax Logical Gated Convolutional Neural Network (SLGCNN) method

The SLGCNN is actually a modification of CNN, particularly for improving the performance of multiple myeloma as an image classification algorithm. SLGCNN is a deep learning-based architecture that extends the basic CNN framework through a logical gating mechanism within the hierarchical architecture of CNN to selectively gated feature maps based on logical conditions instead of storing them. The model applies Softmax activation for the prediction mechanism to enable the classification of multiple myeloma images using probability functions. For the raw network predictions coming out from the previous layers of the same architecture, SLGCNN was applied in the final output layer. It makes it possible to do the multi-class classifications since it makes the total of the output probabilities equal to 1. SLGCNN uses gate control from various layers and integrates them to have a holistic view of image input. The final layer is utilized to classify the image as normal or multiple myeloma-affected or other categories depending on the application. In the equation 17 we perform the convolution operation which is used to extract the features through the used dataset,

$$c_{xy}^{p} = \sum_{m=1}^{M}\sum_{n=1}^{N} i_{(x+m)}^{(p-1)} \cdot u_{mn}^{(p)} + b^{(p)} \quad (17)$$

Let assume, c as output feature map, (x, y) as position, p as layer, i as input image, u as kernel weight, M, N as size of u, and b as bias term. This equation extracts spatial features from input images. After extracts the spatial features we perform logical gating mechanism through equation 18,

$$h(i) = \sigma(u_h . i + b_h) \quad (18)$$

Here, h is represent for the gating function, and σ for sigmoid activation. The logical gating mechanism controls the flow of information by mimicking logical functions like AND, OR, and XOR to enhance feature selection. By following we perform the classification layer and also called as Softmax activation function through the equation 19,

$$Q(j_x|i) = \frac{\exp(c_x)}{\sum_{y=1}^{D}\exp(c_x)} \quad (19)$$

Let assume, Q as Probability, x as class, and D as number of classes. This equation is used to logits (raw scores) into probabilities for each class. After converts raw scores into Q we perform the loss function in equation 20,

$$\mathcal{L} = -\frac{1}{N}\sum_{x=1}^{N}\sum_{y=1}^{D} j_{xy} \log\left(Q(j_y|i_x)\right) \quad (20)$$

This equation is used to measures the difference between the predicted probabilities and the actual labels. In Algorithm 1 we perform the pseudocode of the SLGCNN method,

Algorithm 1:

Input: Set the raw images

Output: Detection of cytoplasm and nucleus cells of multiple myeloma image

Start

For each $R(f_x)$ in image

Use RFE features as input to the SLGCNN

Perform c_{xy}^{p} to extract the features form the used dataset

Accomplish the $h(i)$ to enhance feature selection

End For

Execute the Softmax activation function

$Q(j_x|i) = \frac{\exp(c_x)}{\sum_{y=1}^{D}\exp(c_x)}$ to convert raw scores into probabilities of each class

Evaluate $\mathcal{L}$

Measures the difference between the predicted probabilities and the actual labels

Detect the cytoplasm and nucleus cells

Stop

The presented approach based on the SLGCNN can become a valuable tool for helping doctors diagnose multiple myeloma and increasing the probability of early diagnosis for patients. The SLCNN had higher accuracy because of the logical gating mechanism it used. The methodology proposed here is valuable as the means of developing multiple myeloma image classification tasks. The SLGCNN built with a logical gated type is appropriate for learning and classification because it can effectively solve the difficulties and variants in multiple myeloma images. The softmax activation layer used on the output layer improves the interpretability of

probabilities for the sake of giving more clinically relevant decisions. The use of the proposed SLGCNN for multiple myeloma prediction has shown accurate and reliable performance in the detection of the same.

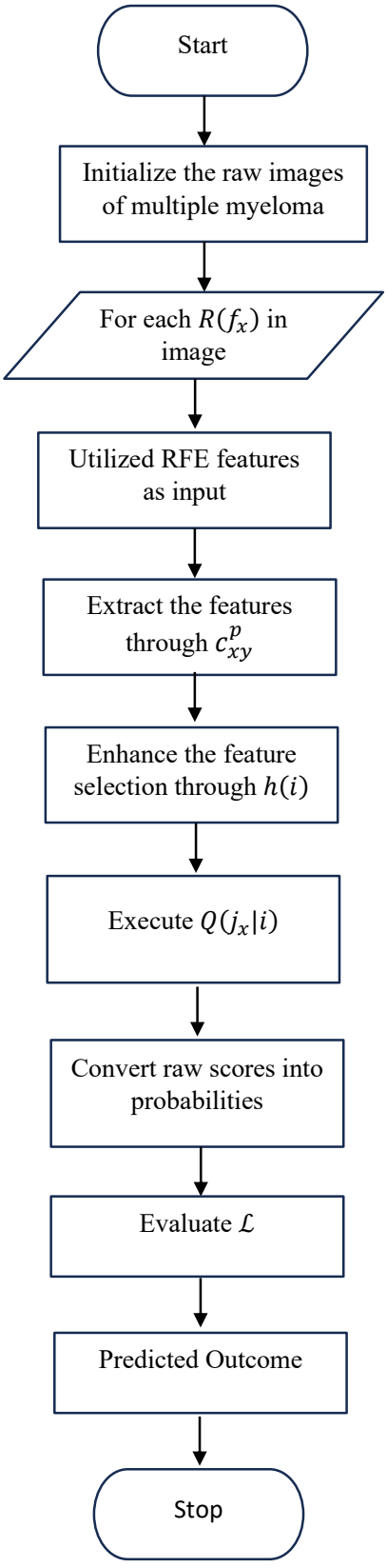

Figure 5. Flowchart Diagram of the SLGCNN method

In Figure 5, we illustrate the workflow diagram of the SLGCNN method. In this method, we first initialize the raw images of multiple myeloma to perform the SLGCNN method. For each $R(f_x)$ in the image, use the RFE features as input, then extract the features through c_{xy}^{p}. After removing the image, we progressed with the feature selection through $h(i)$. Then, we perform the $Q(j_x|i)$ to convert the raw scores into probabilities. Then, we measure the difference between the predicted probabilities and the actual labels through the $\mathcal{L}$, after which we evaluate the L to get the expected outcome, which is cytoplasm and nucleus cells.

4. Result and Discussion

In this section, the proposed SLGCNN method for myeloma prediction using a bone cancer dataset is evaluated using the dataset's incidence and features. Furthermore, the features in the dataset were selected and analyzed based on previous techniques such as FSVM, ANN, and DCNN and the proposed SLGCNN method for multiple myeloma detection. Moreover, bone cancer can be diagnosed by using classification features that represent each image type in the dataset. The performance of the proposed system was evaluated based on the predicted and actual results using a confusion matrix to construct the sensitivity, specificity, F1 score, accuracy, and time complexity for bone cancer prediction.

Table 2. Simulation Parameter

Parameters	Value
Dataset Name	SegPC-2021-dataset
No of Images	575
Training	298
Testing	277
Tool	Jupyter Notebook
Language	Python

Table 3. Performance in Sensitivity

No of Images	FSVM in%	ANN in%	DCNN in%	SLGCNN in %
143	56	59	63	66
286	63	66	68	71
429	67	69	72	75
572	71	73	75	77

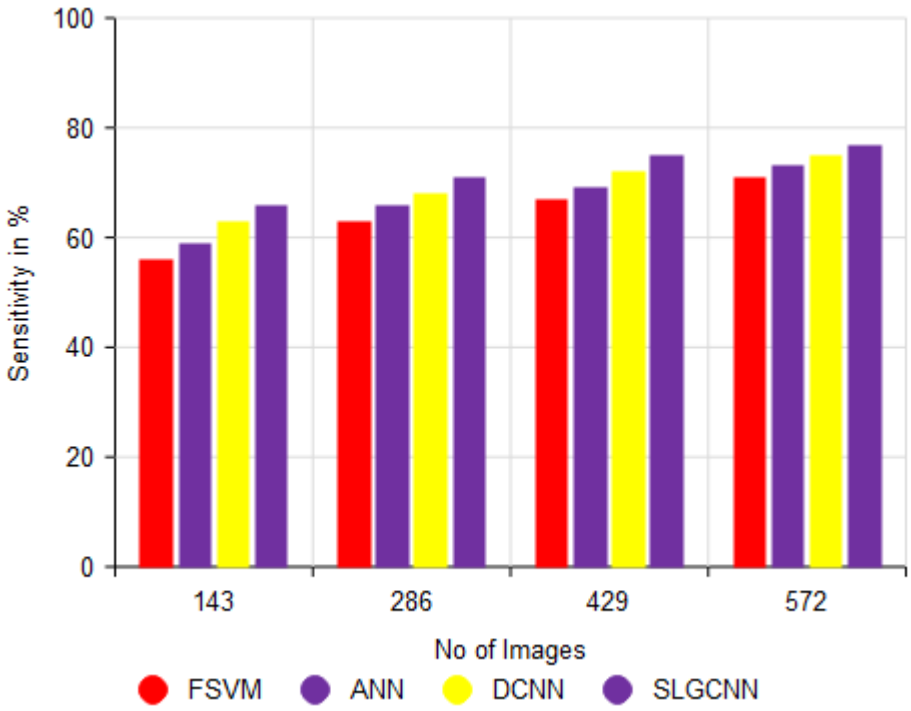

Figure 6. Analysis of Sensitivity

Figure 6 and Table 3 shows that bone cancer can be predicted using a dataset through image processing using sensitivity analysis. The proposed SLGCNN method can classify MM disease images based on the images in the dataset. Furthermore, the proposed SLGCNN has been shown to have a rate of 77% compared to other techniques. Similarly, the sensitivity analysis rates of the proposed method and previous techniques, such as FSVM, ANN, and DCNN, have been described as 71%, 73%, and 75%, respectively.

Table 4. Performance in Specificity

No of Images	FSVM in %	ANN in %	DCNN in %	SLGCNN in%
143	63	66	69	73
286	67	70	74	77
429	71	75	78	81
572	75	79	82	85

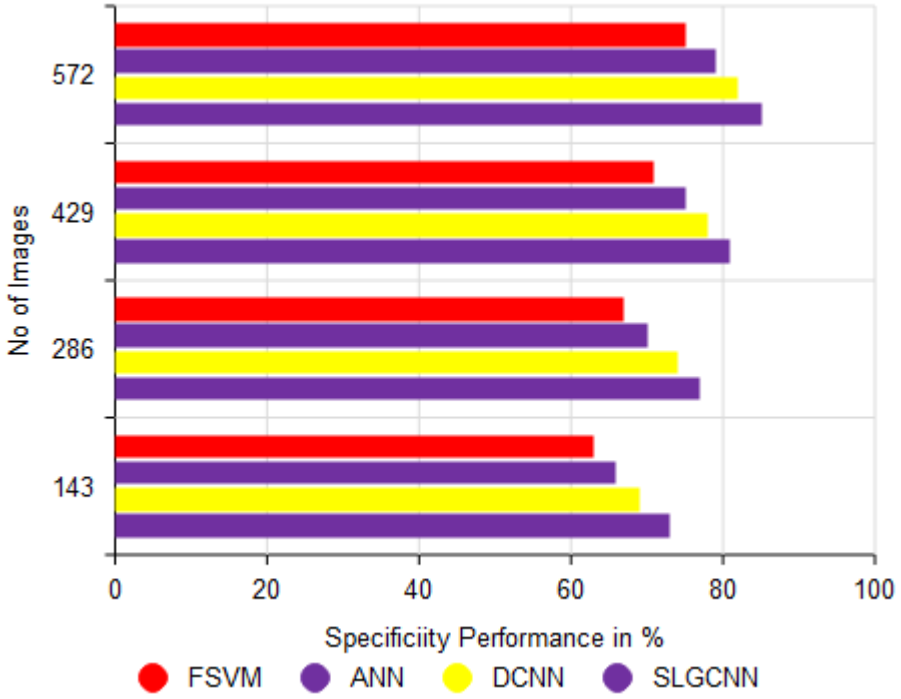

Figure 7. Analysis of Specificity

Figure 7 and Table 4, indicates that bone cancer can be predicted using imaged datasets with specificity analyses. The proposed SLGCNN method can classify multiple myeloma disease images based on images in the dataset. Furthermore, the proposed SLGCNN has been demonstrated to have an accuracy of 85% compared to other methods. Similarly, the specificity analysis rates of the proposed method and the conventional techniques, such as FSVM, ANN, and DCNN, are 75%, 79%, and 82%, respectively.

Table 5. Performance in F1-Score

No of Images	FSVM in %	ANN in %	DCNN in %	SLGCNN in%
143	66	69	74	79
286	70	76	79	85
429	75	79	85	89
572	79	84	89	92

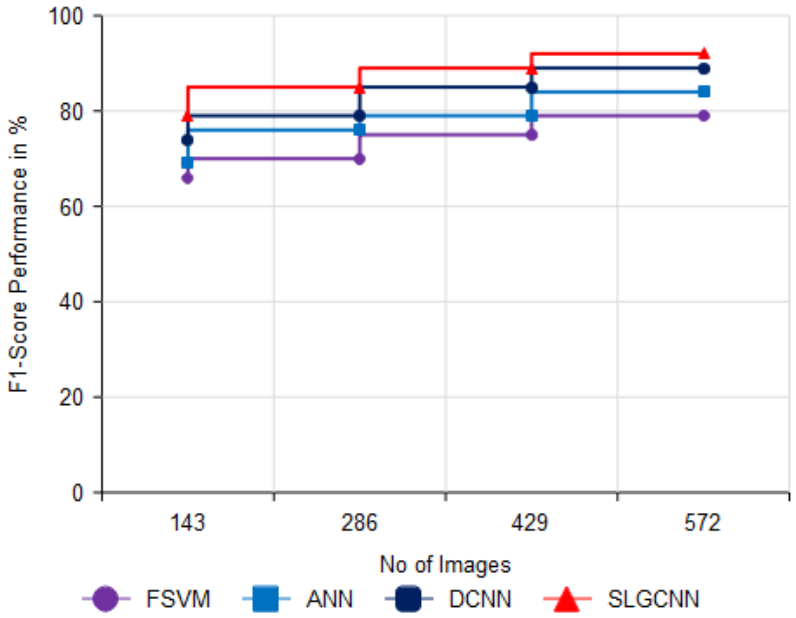

Figure 8. Analysis of F1-Score

Figure 8 and Table 5 shows that image datasets with F1 score analysis can be used for bone cancer prediction. The proposed SLGCNN method can classify multiple myeloma disease images based on images in the dataset. Also, the proposed SLGCNN has been demonstrated to have 92% accuracy compared to other methods. Similarly, the F1-score analysis rates of the proposed method and conventional methods such as FSVM, ANN, and DCNN are 79%, 84%, and 89%, respectively.

Table 6. Performance in Accuracy

No of Images	FSVM in %	ANN in %	DCNN in %	SLGCNN in %
143	71	75	79	83
286	75	79	83	88
429	79	82	87	92
572	83	86	92	96.8

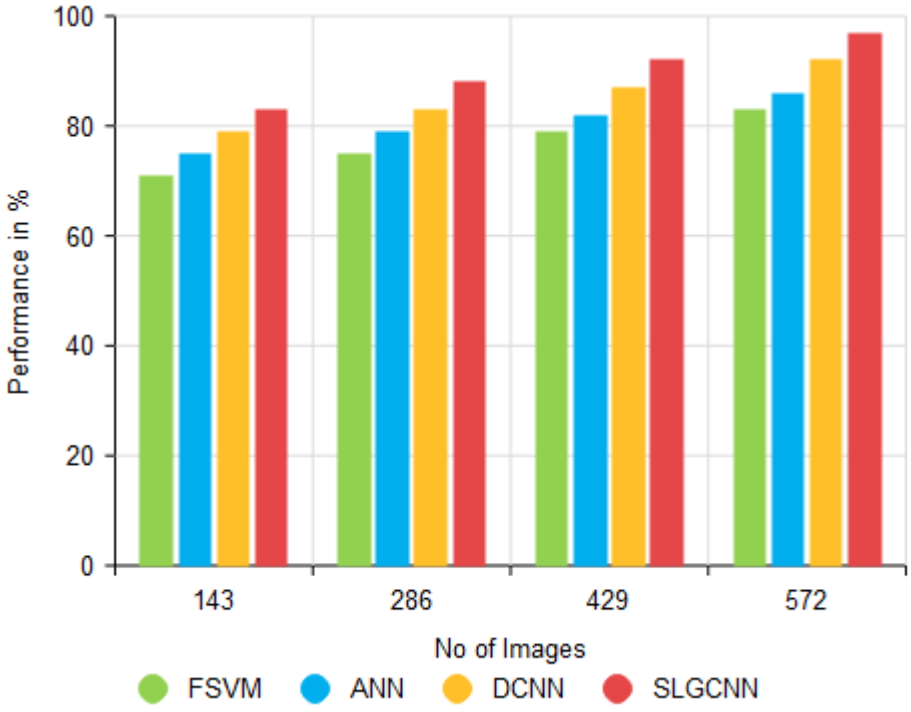

Figure 4. Analysis of Accuracy

As shown in Figure 9 and Table 6, bone cancer can be predicted using the picture dataset that was examined for accuracy. Images from the collection can be used to classify multiple myeloma illness images using the suggested SLGCNN approach. Similarly, this method's accuracy analysis rates are 83%, 86%, and 92%, respectively, compared to the conventional techniques FSVM, ANN, and DCNN. Furthermore, the suggested SLGCNN outperforms other techniques with an accuracy of 96.8%.

Table 7. Performance in Time Complexity

No of Images	FSVM in ms	ANN in ms	DCNN in ms	SLGCNN ms
143	37	33	29	24
286	34	29	24	21
429	30	27	21	17
572	24.9	20.6	18.7	14.3

Figure 10. Analysis of Time Complexity

The bone cancer image collection that was evaluated for time complexity can be used to predict bone cancer, as illustrated in Figure 10 and Table 7. The proposed SLGCNN method can be implemented in the dataset to categorize images of multiple myeloma diseases. Comparing this method to the traditional techniques of ANN, DCNN, and FSVM, the accuracy analysis rates are 18.7ms, 20.6 ms, and 24.9 ms, respectively. Furthermore, with a time complexity of 14.3 ms, the proposed SLGCNN exceeds previous approaches.

5. CONCLUSION

In this study, we employed the SLGCNN technique to accurately categorise multiple myeloma cells as cytoplasm or nucleus. The accuracy of the suggested approach is 96.8%. The MIFED technique is suitable, particularly in medical imaging, to enhance image quality without enhancing the smoothening of crucial structures since it eliminates high-frequency noises like salt and pepper noise. By using a MIFED, the SegPC-2021 dataset helps to improve the overall quality of images for the target disease and ride such deep learning form features associated with the disease. Following preprocessing, we employ SCAS to segment the preprocessed image into more manageable, smaller sections, or "clusters," based on specific attributes or criteria. By matching with actual multiple myeloma locations, the segmented clusters yield a score ranging from 0 (no overlap) to 1 (perfect overlap). The selection of an essential set of features was then accomplished using the RFE approach, which reduced the number of features and sped up processing without sacrificing efficiency. Lastly, we classified multiple myeloma images using the SLGCNN method, providing an accurate and efficient way to identify this type of cancer. It helps to overcome the difficulties caused by the complex visual features of multiple myeloma by discriminating between classes with a high degree of accuracy. With its strong capacity to detect multiple

myeloma accurately, the SLGCNN technique shows promise as a method to support early diagnosis and advance cancer treatment.

REFERENCE

1. Rasch, Stine, et al. "Multiple myeloma associated bone disease." *Cancers* 12.8 (2020): 2113.
2. Ramasamy, M. D., Dhanaraj, R. K., Pani, S. K., Das, R. P., Movassagh, A. A., Gheisari, M., Liu, Y., Porkar, P., & Banu, S. (2022). An improved deep convolutionary neural network for bone marrow cancer detection using image processing. *Informatics in Medicine Unlocked*, *38*, 101233. https://doi.org/10.1016/j.imu.2023.101233
3. Hemminki K, Försti A, Houlston R, Sud A. Epidemiology, genetics and treatment of multiple myeloma and precursor diseases. Int J Cancer. 2021 Dec 15;149(12):1980-1996. doi: 10.1002/ijc.33762. Epub 2021 Aug 30. PMID: 34398972; PMCID: PMC11497332.
4. Chen X, Zhang Y, Li X, Yang Z, Liu A, Yu X. Diagnosis and staging of multiple myeloma using serum-based laser-induced breakdown spectroscopy combined with machine learning methods. Biomed Opt Express. 2021 May 21;12(6):3584-3596. doi: 10.1364/BOE.421333. PMID: 34221680; PMCID: PMC8221939.
5. Pourhanifeh, M. H., Mahjoubin-Tehran, M., Shafiee, A., Hajighadimi, S., Moradizarmehri, S., Mirzaei, H., & Asemi, Z. (2020). MicroRNAs and exosomes: Small molecules with big actions in multiple myeloma pathogenesis. *IUBMB Life*, *72*(3), 314-333. https://doi.org/10.1002/iub.2211
6. Ban, C.; Yang, F.; Wei, M.; Liu, Q.; Wang, J.; Chen, L.; Lu, L.; Xie, D.; Liu, L.; Huang, J. Integrative Analysis of Gene Expression Through One-Class Logistic Regression Machine Learning Identifies Stemness Features in Multiple Myeloma. *Front. Genet.* **2021**, *12*.
7. Robak P, Dróżdż I, Jarych D, Mikulski D, Węgłowska E, Siemieniuk-Ryś M, Misiewicz M, Stawiski K, Fendler W, Szemraj J, Smolewski P, Robak T. The Value of Serum MicroRNA Expression Signature in Predicting Refractoriness to Bortezomib-Based Therapy in Multiple Myeloma Patients. Cancers (Basel). 2020 Sep 9;12(9):2569. doi: 10.3390/cancers12092569. PMID: 32916955; PMCID: PMC7565855.
8. Allegra A, Ettari R, Innao V, Bitto A. Potential Role of microRNAs in inducing Drug Resistance in Patients with Multiple Myeloma. Cells. 2021 Feb 20;10(2):448. doi: 10.3390/cells10020448. PMID: 33672466; PMCID: PMC7923438.
9. Hansford BG, Silbermann R. Advanced Imaging of Multiple Myeloma Bone Disease. Front Endocrinol (Lausanne). 2018 Aug 7; 9:436. doi: 10.3389/fendo.2018.00436. PMID: 30131767; PMCID: PMC6090033.
10. Gehlot, Shiv, Anubha Gupta, and Ritu Gupta. "A CNN-based unified framework utilizing projection loss in unison with label noise handling for multiple Myeloma cancer diagnosis." Medical Image Analysis 72 (2021): 102099
11. Reem A. Almulhim, 2022. "Multiple Myeloma. Detection from Histological Images Using Deep Learning," Eximia Journal, Plus Communication Consulting SRL, vol. 5(1), pages 113-145, July.
12. Rasal T, Veerakumar T, Subudhi BN, Esakkirajan S. Segmentation and counting of multiple myeloma cells using IEMD based deep neural network. Leuk Res. 2022 Nov; 122:106950. doi: 10.1016/j.leukres.2022.106950. Epub 2022 Sep 7. PMID: 36152502.
13. Jinxia He, Kaifeng Zhang, "Medical image analysis of multiple myeloma based on the convolutional neural network", Volume 39, Issue 3, 12 September 2021, https://doi.org/10.1111/exsy.12810.
14. Wang, Jinzhou, et al. "Deep Learning-Based CT Imaging in Diagnosing Myeloma and Its Prognosis Evaluation." *Journal of Healthcare Engineering* 2021.1 (2021): 5436793.
15. Faghani, S., Baffour, F.I., Ringler, M.D. *et al.* A deep learning algorithm for detecting lytic bone lesions of multiple myeloma on CT. *Skeletal Radiol* **52**, 91–98 (2023). https://doi.org/10.1007/s00256-022-04160-z.
16. Janasruti, U., et al. "Deep Learning-Based Approach to Detect Leukemia, Lymphoma, and Multiple Myeloma in Bone Marrow." *AI-Enabled Smart Healthcare Using Biomedical Signals*. IGI Global, 2022. 259-282.
17. Mosquera Orgueira, Adrián, et al. "Survival prediction and treatment optimization of multiple myeloma patients using machine-learning models based on clinical and gene expression data." *Leukemia* 35.10 (2021): 2924-2935.
18. Venkatachalam Kandasamy, Vladimir Simic, Nebojsa Bacanin, Dragan Pamucar, "Optimized deep learning networks for accurate identification of cancer cells in bone marrow," Neural Networks, Volume 181, 2025, 106822, ISSN 0893-6080, https://doi.org/10.1016/j.neunet.2024.106822.
19. D. Kumar et al., "Automatic Detection of White Blood Cancer from Bone Marrow Microscopic Images Using Convolutional Neural Networks," in IEEE Access, vol. 8, pp. 142521-142531, 2020, doi: 10.1109/ACCESS.2020.3012292.

20. Shiv Gehlot, Anubha Gupta, Ritu Gupta, "A CNN-based unified framework utilizing projection loss in unison with label noise handling for multiple Myeloma cancer diagnosis," Medical Image Analysis, Volume 72, 2021, 102099, ISSN 1361-8415, https://doi.org/10.1016/j.media.2021.102099.
21. Zbigniew Omiotek, Olga Stepanchenko, Waldemar Wójcik, Wojciech Legieć, Małgorzata Szatkowska, "The use of the Hellwigs method for feature selection in the detection of myeloma bone destruction based on radiographic images," Biocybernetics and Biomedical Engineering, Volume 39, Issue 2, 2019, Pages 328-338, ISSN 0208-5216, https://doi.org/10.1016/j.bbe.2018.11.008.
22. Shobana M, Balasraswathi VR, Radhika R, Oleiwi AK, Chaudhury S, Ladkat AS, Naved M, Rahmani AW. Classification and Detection of Mesothelioma Cancer Using Feature Selection-Enabled Machine Learning Technique. Biomed Res Int. 2022 Jul 27;2022:9900668. doi: 10.1155/2022/9900668. Retraction in: Biomed Res Int. 2024 Jan 9; 2024:9868791. doi: 10.1155/2024/9868791. PMID: 35937383; PMCID: PMC9348925.
23. Guilal, Rima, et al. "Feature importance analysis for a highly unbalanced multiple myeloma data classification." *International Journal of Medical Engineering and Informatics* 16.3 (2024): 199-209.
24. Cai, Jiangying, et al. "Construction of the prediction model for multiple myeloma based on machine learning." *International Journal of Laboratory Hematology* (2024).
25. Aarthy, R., V. Muthupriya, and G. N. Balaji. "Detection of bone cancer based on a four-phase framework generative deep belief neural network in deep learning." *Alexandria Engineering Journal* 109 (2024): 394-407.
26. Yu, Ta-Chuan, et al. "A machine-learning-based algorithm for bone marrow cell differential counting." *International Journal of Medical Informatics* (2024): 105692.
27. Xiong X, Wang J, Hu S, Dai Y, Zhang Y, Hu C. Differentiating Between Multiple Myeloma and Metastasis Subtypes of Lumbar Vertebra Lesions Using Machine Learning-Based Radiomics. Front Oncol. 2021 Feb 24; 11:601699. doi: 10.3389/fonc.2021.601699. PMID: 33718148; PMCID: PMC7943866.
28. Ubels J, Sonneveld P, van Vliet MH, de Ridder J. Gene Networks Constructed Through Simulated Treatment Learning can Predict Proteasome Inhibitor Benefit in Multiple Myeloma. Clin Cancer Res. 2020 Nov 15;26(22):5952-5961. doi: 10.1158/1078-0432.CCR-20-0742. Epub 2020 Sep 10. PMID: 32913136.
29. Reinert, Christian Philipp, et al. "Role of computed tomography texture analysis using dual-energy-based bone marrow imaging for multiple myeloma characterization: comparison with histology and established serologic parameters." *European Radiology* 31 (2021): 2357-2367.
30. Kumar, Deepika, et al. "Automatic detection of white blood cancer from bone marrow microscopic images using convolutional neural networks." *IEEE Access* 8 (2020): 142521-142531.